WILEY-VCH

DOI: 10.1002/((please add manuscript number))
Article type: Communication

An electrocorticography device with an integrated microfluidic ion pump for simultaneous neural recording and electrophoretic drug delivery *in vivo*

Christopher M. Proctor[1,5,+], Ilke Uguz[2,5,+], Andrea Slezia[3], Vincenzo Curto[1,5], Sahika Inal[4,5], Adam Williamson[3], and George G. Malliaras[1,5*]*

[1]Dr. C.M. Proctor, Dr. V. Curto, Prof. G.G. Malliaras.
Department of Engineering, University of Cambridge, CB3 0FA, United Kingdom

[2]Dr. I. Uguz.
Department of Electrical Engineering, Colombia University, New York, NY 10027

[3]Dr. A. Slezia, Dr. A. Williamson

Aix Marseille Université, INS, UMR_S 1106, 13005 Marseille, France

[4]Prof. S. Inal
Biological and Environmental Science and Engineering, King Abdullah University of Science and Technology (KAUST), Thuwal 23955-6900, Saudi Arabia

[5]Dr. C.M. Proctor, Dr. I Uguz, Dr. V. Curto, Dr. S. Inal, Prof. G.G. Malliaras.
Department of Bioelectronics, Ecole Nationale Superieure des Mines, CMP-EMSE, MOC, 13541 Gardanne, France

[+]equal contribution
*Corresponding e-mail: gm603@cam.ac.uk and adam.williamson@univ-amu.fr

Keywords: ((neuroengineering, drug delivery, electrocortigraphy, electrophoretic, bioelectronics))

Abstract: ((The challenge of treating neurological disorders has motivated the development of implantable devices that can deliver treatment when and where it's needed. This study presents a novel brain implant capable of electrophoretically delivering drugs and recording local neural activity on the surface of the brain. The drug delivery is made possible by the integration of a microfluidic ion pump (µFIP) into a conformable electrocorticography (ECoG) device with recording cites embedded next to the drug delivery outlets. The µFIP ECoG device can deliver a high capacity of several biologically important cationic species on demand. The therapeutic potential of the device is demonstrated by using it to deliver

neurotransmitters in a rodent model while simultaneously recording local neural activity. These developments represent a significant step forward for cortical drug-delivery systems.))

Implantable devices for localized drug delivery have attracted much interest for the treatment neurological disorders due to the difficulty of systemically delivering drugs across the blood brain barrier (BBB). Such localized drug delivery also promises fewer side effects compared to systemic drug treatments as systemically administered drugs often interact with healthy regions of the body. Implants that do not penetrate the brain are in many cases preferable to brain-penetrating ones, as the latter cause more tissue damage and increase risk for the patient. To that end, there have been multiple devices designed for drug delivery within the intracranial space between brain and skull including gels and tablets that release drugs as they dissolve and various systems that allow for fluidic injection of drug [1–3]. However, fluidic drug injection systems have been plagued by problems with clogging and reflux [4,5] while the single-use nature of dissolving implants is not well suited for the treatment of chronic disorders.

An alternative approach in which drugs are delivered on demand by electrophoresis across an ion conducting membrane from a fluidic reservoir has shown potential to overcome the above problems [6–8]. Electrophoretic drug delivery offers the advantage of precise spatial and temporal control of drug delivery while avoiding issues with clogging or reflux. Devices that electrophoretically deliver drugs have already been used to treat pain[9], cancerous tumours[8], and seizure like activity [10–12]. The recent development of the microfluidic ion pump design (μFIP) has furthered these efforts by significantly reducing the electric potential needed to deliver drugs [13]. Equally important is the demonstration that such devices can work in tune with imbedded recording electrodes or other biosensors to optimize the treatment a milestone that was first demonstrated *in vitro*[10,14] and then *in vivo* using a μFIP depth probes with two recording sites[12]. In terms of cortical drug delivery, the incorporation of recording electrodes

for real time analysis of local neural activity would be particularly beneficial as electrocortigraphy (ECoG) devices are already an established clinical tool for diagnosing disorders such as epilepsy [15,16] Moreover, ECoG devices have quickly evolved in recent years by taking advantage of ultra-conformable substrates and conducting polymer coatings to expand the limits of what can be learned from cortical recordings[17,18].

In this work, we combine the design principles from state-of-the-art ECoG devices and electrophoretic drug delivery devices to present a cortical device that can simultaneously deliver drugs and record local neural activity. This represents a significant advancement in cortical devices for neural interfacing as the ability to monitor neural activity in real time can greatly enhance the efficacy of drug treatment regimens[19,20]. The device design is presented in **Figure 1** with arrows and text marking the primary components including the electrode pads for connecting to an external recording system, the source and target pads for connecting to the source and target electrodes of the μFIP as well as the fluidic inlet/outlet for loading/exchanging the drug solution (see Experimental Section for fabrication details). As can be seen in the full device picture and the cross section, a microfluidic channel runs length wise across the device between the fluidic inlet and outlets with the μFIP source electrode placed at the bottom of the microfluidic channel. The purpose of the microfluidic channel is to transport the drug in solution to the drug delivery outlets thereby reducing the distance and hence the applied potential needed to pump the drug across to the tissue where the device is implanted[13]. The microfluidic channel also serves as reservoir for the drug of interest which can be readily exchanged using standard microfluidic connections. As shown in the upper left image of Figure 1, the active area (approx. 3 mm^2) features a central region with the μFIP drug delivery outlets – a grid of 300 holes, 10 μm in diameter, coated with a ca. 6 um thick polystyrene sulfonate based ion bridge material that selectively transports cations [11,13] (see Experimental). The ion pump outlets are flanked by 32 PEDOT:PSS/Au recording sites each 15 μm x 15 μm thereby enabling high fidelity recordings with excellent signal to noise ratio

from the immediate area surrounding the drug delivery outlets. The recording sites are surrounded by the U-shaped target PEDOT:PSS/Au electrode for the µFIP with a surface area of approx. 2.5 mm^2. The high volumetric capacitance of the PEDOT:PSS coating on the target and source electrodes significantly increases the drug delivery capacity of the µFIP relative to standard polarizable electrodes of equivalent area (ie. Au, Pt, etc) [6,21].

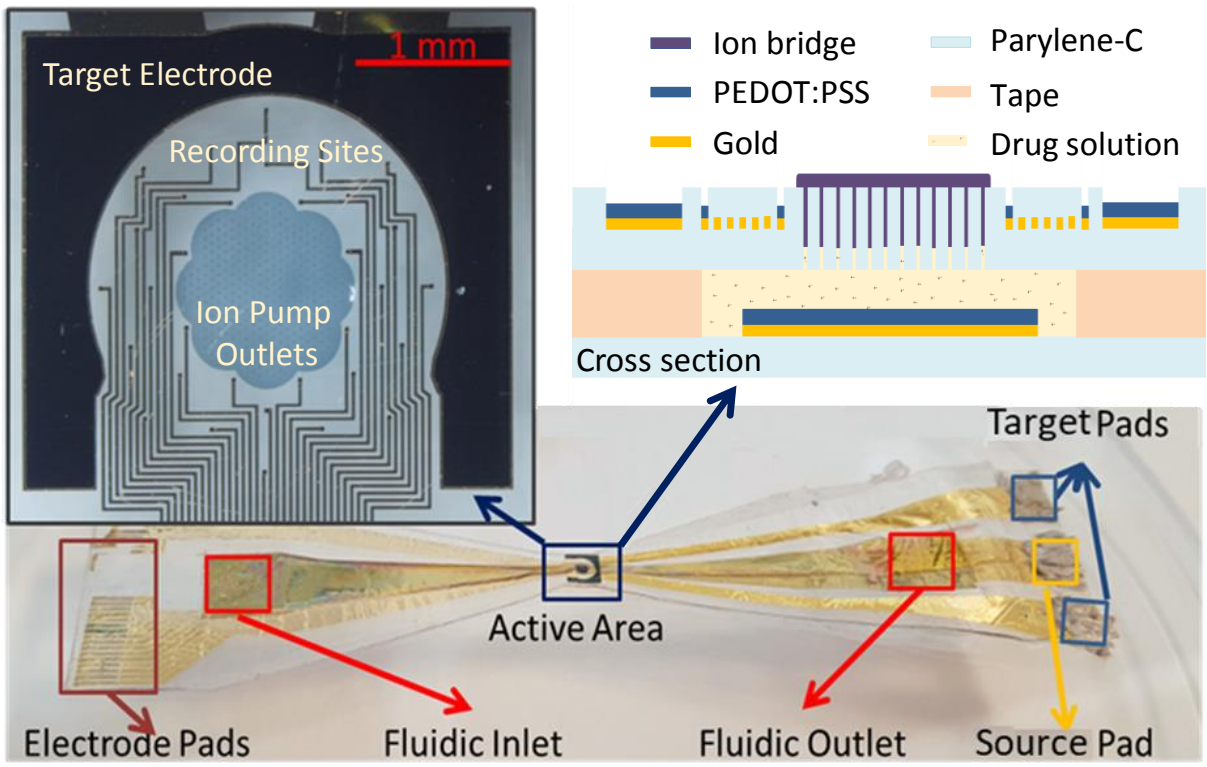

Figure 1: Photograph of the electrocortigraphy device with labelled components including a close up image of the active area featuring the ion pump target electrode, recording sites and the ion pump drug delivery outlets. A schematic cross section of the device along the central axis of the active area is also shown.

The drug delivery capacity of the device was explored for the delivery of H+, K+, acetylcholine and gamma amino butyric acid (GABA). These cations can be selectively delivered with the PSS based ion bridge and each serves important roles in the brain. For instance, potassium is an essential ion that determines cell membrane potential and GABA is an inhibitory neurotransmitter that that regulates communication between brain cells. Acetylcholine is a neurotransmitter that contributes to many functions including muscle

actuation and learning. Local changes or deficiencies in the concentration of each of these ions has been tied to neurological problems that include Alzheimer's disease[22], epilepsy[23], glioblastoma[24] and traumatic brain injury[25]. In order to test the drug delivery capacity in physiological conditions, the microfluidic channel was loaded with solutions containing the drug of interest and the active area was immersed into a phosphate buffered saline solution (see Experimental section). The total charge pumped as a function of time with an applied potential of 0.5 V between the source and target electrodes is shown in **Figure 2**. For all cations, the net charge delivered rises rapidly in the initial seconds of delivery then continues at a reduced rate as the source and target electrodes become increasingly polarized as is typical for capacitive based electrophoretic drug delivery devices [6,13,26]. The trend in net charge delivered was found to correlate with the size of the cation with more than double the amount of charge delivered for the smallest ion (H+) compared to the largest (GABA). This can be understood by considering that the μFIP current is directly proportional to the ionic mobility which generally decreases with increasing size of the ionic species [27,28]. To put the drug delivery capacity into context, the net charge was converted to moles of cation delivered (Fig 2, right y axis) by taking the lower limit of the previously demonstrated pumping efficiency of 90% for this thickness of PSS based ion bridge [13]. For instance, it can be seen that this device can deliver upwards of 0.5 nmol of GABA in just 30 seconds. In contrast, our recently reported μFIP depth probe requires 30 minutes of continuous delivery and double the applied potential to deliver the equivalent amount of GABA[12]. The improvement in drug delivery capacity/rate for the ECoG device can be explained by the increase in capacitance of the source/target electrodes as well as the larger surface area for drug delivery. This increased capacity is likely to be essential to the success of cortical drug delivery as the delivered drug may need to diffuse further into tissue in order to reach the desired target compared to more invasive drug delivery devices that penetrate the brain.

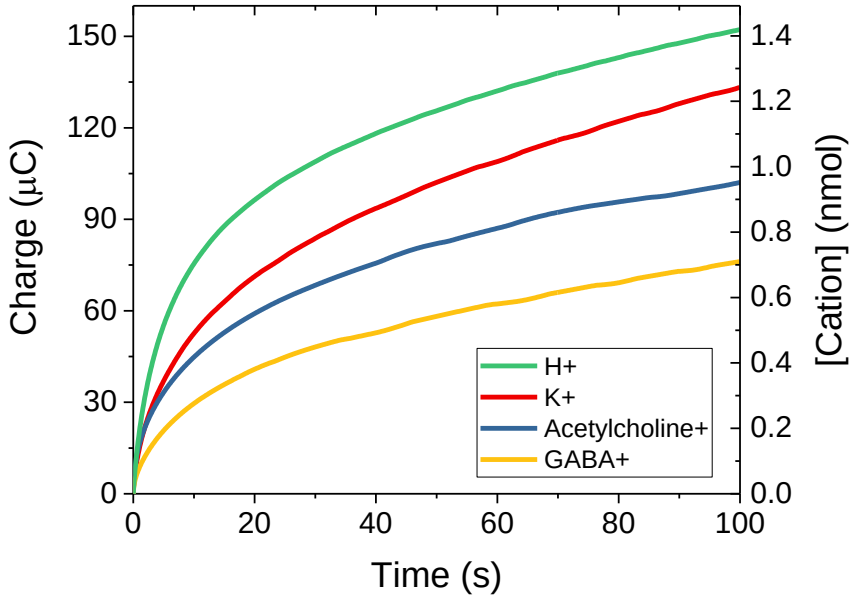

Figure 2: Total charge and number of cations delivered from source to target as a function of time with an applied voltage of 0.5 V for various physiologically important cations.

Equally important to the viability of this device is the performance of the recording electrodes. As an initial test, the impedance of the recording sites was measured before and after operation of the µFIP. The average impedance for the recording sites was 7 kOhm at 1 kHz (Figure S1) consistent with previous reports of PEDOT:PSS coated recording sites of similar dimensions[29,30] and no change was observed following operation of the µFIP.

After validating the performance in physiological conditions, the active area of the ECoG device was implanted on the cortex of an anaesthetized mouse. The purpose of the in vivo testing was to explore the capability of the device to simultaneously record and deliver drugs and to perform a preliminary test of the therapeutic potential of cortical drug delivery to address seizure like events (SLEs) which are characteristic of epilepsy. The implantability was readily confirmed as the flexible nature allowed for conformal covering of the exposed cortex with the active area of the device. The ability to record and deliver drugs was also evident. Representative recordings from recording sites within three distinct regions of the

device surrounding the drug delivery outlets are shown in the centre right panel of **Figure 3** with the recording site locations noted with red circles/text on the image of the active area. A green arrow marks the start of a 100 second period of electrophoretic delivery of GABA from the μFIP (0.5 V applied between the source and target electrodes). The recordings were not noticeably affected by the operation of the μFIP thereby allowing for continuous recordings before during, and after, drug delivery. Also, of note is that there are subtle differences in the time-synchronized recordings of the electrical activity measured by each recording site which demonstrates the ability of each site to capture local activity. This is most evident in the high-resolution clips shown for shorter time scales above and below recording sites A and C respectively.

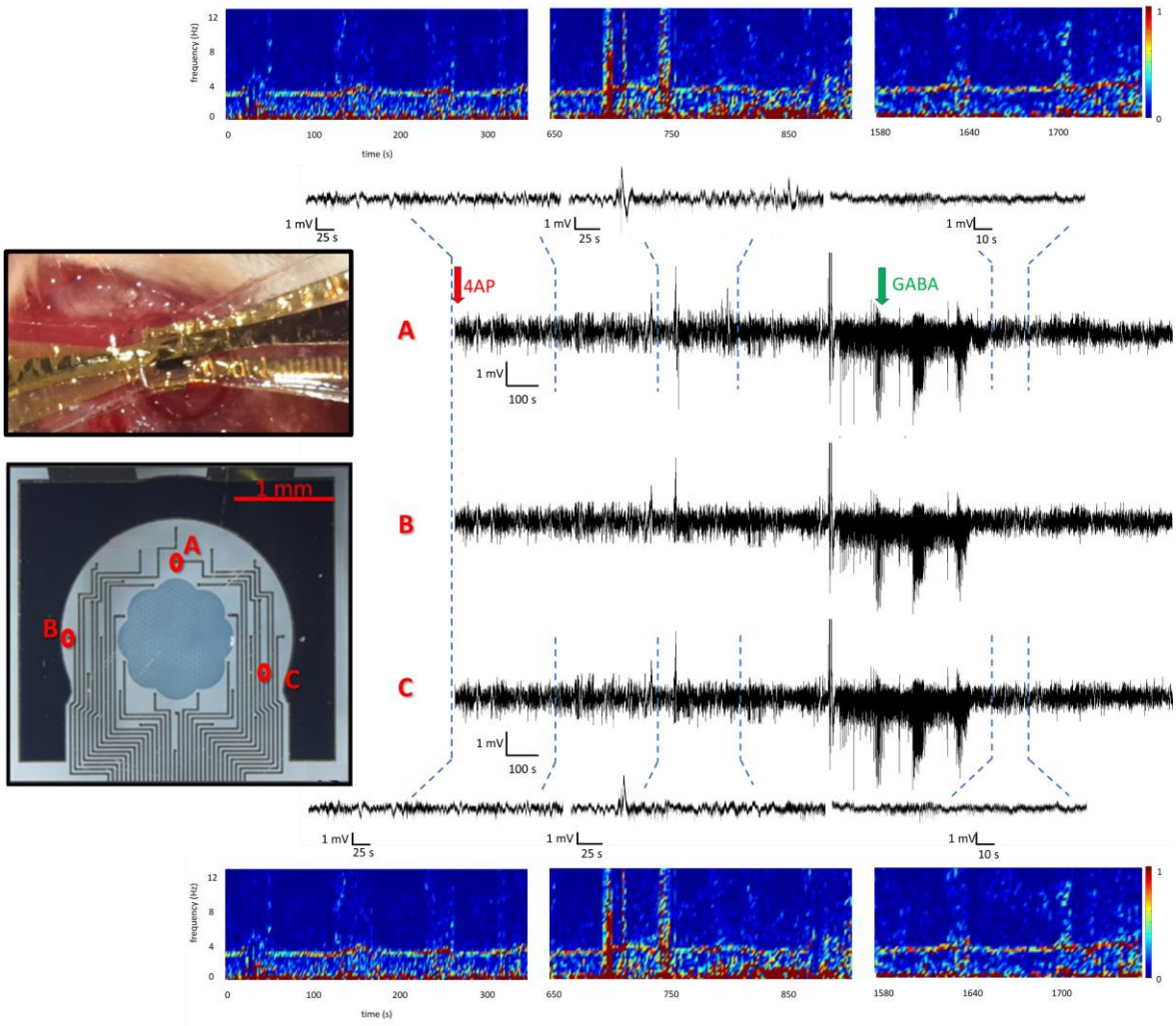

Figure 3: Representative recordings from three different recording sites (circled in red) for an experiment in an anesthetized mouse before, during, and after injection of 4AP (noted by red arrow). Green arrow marks the start of electrophoretic delivery of GABA using the ion pump. The top and bottom panels feature time/frequency plots and high resolution clips of the recordings on shorter time scales for three critical time ranges (as noted by dashed arrows) for electrodes A and C.

Beyond showing the ability to record and delivery drugs, the results in Figure 3 hint at the therapeutic potential of electrophoretic drug delivery for treating epilepsy that is focal to the cortex. This form of pathology is not uncommon in focal cortical dysplasia one of the most common causes of drug-resistant epilepsy[31,32]. Considering surgical resection is often the only treatment option for these patients, a cortical drug delivery device such as the μFIP ECoG presented here could be of tremendous benefit if it proved effective for seizure control. Upon implanting the ECoG device, a concentrated dose of 4-aminopyridine (4AP) known to induce intense seizure like events [33,34] was injected into the top layer of the cortex directly beneath the active area of the device (see Experimental Section). The upper and lower panels in Figure 3 highlight three regions of the recordings with high resolution clips and time/frequency analysis for recordings sites A and C. In the first region, both recording sites show normal physiological activity with sub 4 Hz frequencies consistent with anaesthesia. In the second region, the effects of the 4AP are evident with the observation of interictal spikes seen in the time/frequency plots as higher frequency activity. Notably, the interictal spikes on recording site C are monophasic while they are biphasic with higher amplitude in recording site A suggesting that recording site A may be in closer proximity to a source/sink point of the pathology induced by the 4AP injection. Approximately 300 s after the first interictal spikes, a seizure like event (SLE) was observed marked by continuous high frequency activity (>5 Hz). The electrophoretic delivery of GABA was then initiated (green arrow) for a period of 100 s. Roughly 250 seconds after the initiation of GABA delivery, the activity in all recording sites

returned to lower frequencies consistent with normal physiological activity under anaesthesia with no further observations of pathological activity. Control experiments without GABA delivery using similar doses of 4AP typically resulted in multiple SLE events lasting upwards of two hours (see Fig S2) which is notably longer than the period of pathological events observed in the two trials in which GABA was delivered with the μFIP ECoG. This suggests that electrophoretic delivery of GABA to the cortex may be able to have similar effect on cortical seizures as it was found to have in the hippocampus [11,12]. While these results are encouraging, further research will be required in order to fully assess the efficacy of electrophoretic drug delivery for addressing cortical focused epilepsy. To that end, of particular interest will be to take advantage of the μFIPs ability to readily tune the timing, location and dosing of drug delivery in order to optimize treatment.

Looking ahead to future applications, in addition to addressing some forms of epilepsy, we postulate that the μFIP ECoG may find utility as a tool for understanding and treating traumatic brain injuries (TBIs) and as a component in brain-machine interfaces. For instance, an implanted μFIP ECoG could provide critical insight into brain activity following a TBI and offer a means to deliver therapeutic agents as needed. These efforts will be aided by the fact that the device design presented here can readily incorporate alternative ion bridge materials to expand the library of deliverable drugs[27,35]. Likewise, the incorporation of additional backend electronics can enable closed loop feedback and control such that the μFIP can respond automatically to the input from the recording sites and/or other onboard biosensors [20,36–38]. Future research will focus on remaining technological and scientific challenges including developing new ion bridge materials, validating the long-term efficacy and stability of μFIP ECoG devices and investigating the therapeutic capabilities in appropriate disease models. We anticipate these efforts will enable μFIP ECoG devices to be introduced to the clinic within a decade.

In summary, we have presented an implantable electrocortigraphy device capable of electrophoretically delivering drugs and recording local neural activity on the surface of the brain. The drug delivery is made possible by the integration of a microfluidic ion pump into a conformable ECoG device with recording cites embedded next to the drug delivery outlets. The μFIP ECoG device was shown to be capable of delivering a high capacity of several biologically important cationic species. The therapeutic potential of the device was further demonstrated by using it to deliver neurotransmitters in a rodent model while simultaneously recording local neural activity. These developments represent a significant step forward for cortical drug-delivery systems.

Experimental Section

Device fabrication: The μFIP ECoG devices were constructed following previously reported procedures[13]. In short, the fabrication involved standard photolithography processes to separately fabricate the top and bottom parylene based layers. In the final steps, the top and bottom layers were stuck together with the help of 80 μm medical-grade double adhesive tape (1500 transparent polyethylene, 3M), cut to the shape of the microfluidic channel using a flatbed plotter (FC2250, Graphtec). The primary difference here versus the fabrication in ref. 13 was inclusion of recording electrodes in the top layer. This was achieved using a custom designed photolithography mask (Selba) to pattern the interconnects and electrode pads on the top layer. Connections to the microfluidic inlet/outlet were made using standard rubber adhesive fluidic connectors with a hole punched to match polyethylene tubing (PE-60, Linton Instrumentation).

Device characterization: A Keithley 2612A SourceMeter unit with customized Labview software was used to apply 0.5 V between source and target electrodes while measuring the current. Solutions for each cationic drug of interest were prepared with a concentration of 10 mM in deionized water and then loaded into the microfluidic channel. The microfluidic

channel was flushed with deionized water before and after each drug solution. The device was operated for at least 300 seconds at 0.5 V after loading each drug solution to ensure residual ions from were flushed out of the ion bridge prior to measuring the drug delivery capacity for each drug. For drug delivery capacity measurements, the active area of the device was submerged in artificial cerebral spinal fluid (ACSF).

in vivo experiments: All protocols have been approved by the Institutional Animal Care and Use Committee of INSERM. Adult male *OF1* mice were used for the experiments. Mice were entrained to a 12 h light/dark cycle with food and water available *ad libitum*. All experimental procedures were performed according to the ethical guidelines of the Institut de Neuroscience des Systèmes and approved by the local Ethical Committees and Veterinary Offices. Surgeries and experiments were done under ketamine/xylazine anesthesia (ketamine, 100 mg/kg; xylazine, 10 mg/kg, body weight). Mice were fixed in a mouse stereotaxic frame (Kopf Instruments, CA, USA). After a subcutaneous injection of a local pain killer ropivacaine, craniotomies were performed on the head-fixed anesthetized mice from bregma: anteroposterior 1.0 mm and mediolateral 1.2 mm; dorsoventral 2.8 mm from the surface). Skull was opened, dura was removed, a Hamilton syringe for 4-AP injection (250 nl of 25 mM in ACSF) with a borosilicate glass capillary (50-100 µm diamter tip) was lowered approxiamtely 100 µm into the cortex. The µFIP ECoG was loaded with a 0.05 M solution of GABA and the active area of the device was placed directly onto the exposed cortex. Fluidic connections were not maintained during the *in vivo* experiments. Neural recordings were made with a 64-channel Neurolynx amplifier (Neurolynx, Montana, USA) using a custom made ZiF to omnetics connector to connect the recording pads on the EcoG to the headstage. Time/frequency plots were made using standard MATLAB script.

Statistical analysis: No statistical analysis was performed in this study.

Supporting Information

Supporting Information is available from the Wiley Online Library or from the author.

Acknowledgements

CMP and IU contributed equally to this work. The authors thank Dr. Christophe Bernard for providing facilities for the *in vivo* experiments. CMP acknowledges funding from a Whitaker International Scholar grant administered by the Institute for International Education. A.W. acknowledges funding from the European Research Council (ERC) under the European Union's Horizon 2020 research and innovation programme (grant agreement No 716867) as well *as* Excellence Initiative of Aix-Marseille University - A*MIDEX, a French "Investissements d'Avenir" programme.

Received: ((will be filled in by the editorial staff))
Revised: ((will be filled in by the editorial staff))
Published online: ((will be filled in by the editorial staff))

References

[1] N. Ludvig, G. Medveczky, J. A. French, C. Carlson, O. Devinsky, R. I. Kuzniecky, "Evolution and Prospects for Intracranial Pharmacotherapy for Refractory Epilepsies: The Subdural Hybrid Neuroprosthesis," DOI 10.1155/2010/725696can be found under https://www.hindawi.com/journals/ert/2010/725696/, **2010**.
[2] N, O. Ludvig, *J. Exp. Stroke Transl. Med.* **2010**, *3*, 13.
[3] H. Kaurav, D. N. Kapoor, *Ther. Deliv.* **2017**, *8*, 1097.
[4] D. S. Bidros, J. K. Liu, M. A. Vogelbaum, *Future Oncol.* **2009**, *6*, 117.
[5] A. Jahangiri, A. T. Chin, P. M. Flanigan, R. Chen, K. Bankiewicz, M. K. Aghi, *J. Neurosurg.* **2017**, *126*, 191.
[6] J. Isaksson, P. Kjäll, D. Nilsson, N. Robinson, M. Berggren, A. Richter-Dahlfors, *Nat. Mater.* **2007**, *6*, 673.
[7] D. T. Simon, S. Kurup, K. C. Larsson, R. Hori, K. Tybrandt, M. Goiny, E. W. H. Jager, M. Berggren, B. Canlon, A. Richter-Dahlfors, *Nat. Mater.* **2009**, *8*, 742.
[8] J. D. Byrne, M. N. R. Jajja, A. T. O'Neill, L. R. Bickford, A. W. Keeler, N. Hyder, K. Wagner, A. Deal, R. E. Little, R. A. Moffitt, C. Stack, M. Nelson, C. R. Brooks, W. Lee, J. C. Luft, M. E. Napier, D. Darr, C. K. Anders, R. Stack, J. E. Tepper, A. Z. Wang, W. C. Zamboni, J. J. Yeh, J. M. DeSimone, *Sci. Transl. Med.* **2015**, *7*, 273ra14.
[9] A. Jonsson, Z. Song, D. Nilsson, B. A. Meyerson, D. T. Simon, B. Linderoth, M. Berggren, *Sci. Adv.* **2015**, *1*, e1500039.
[10] A. Jonsson, S. Inal, I. Uguz, A. J. Williamson, L. Kergoat, J. Rivnay, D. Khodagholy, M. Berggren, C. Bernard, G. G. Malliaras, D. T. Simon, *Proc. Natl. Acad. Sci.* **2016**, *113*, 9440.
[11] A. Williamson, J. Rivnay, L. Kergoat, A. Jonsson, S. Inal, I. Uguz, M. Ferro, A. Ivanov, T. A. Sjöström, D. T. Simon, M. Berggren, G. G. Malliaras, C. Bernard, *Adv. Mater.* **2015**, *27*, 3138.
[12] C. M. Proctor, A. Slézia, A. Kaszas, A. Ghestem, I. del Agua, A.-M. Pappa, C. Bernard, A. Williamson, G. G. Malliaras, *Sci. Adv.* **2018**, *4*, eaau1291.
[13] Uguz Ilke, Proctor Christopher M., Curto Vincenzo F., Pappa Anna-Maria, Donahue Mary J., Ferro Magali, Owens Róisín M., Khodagholy Dion, Inal Sahika, Malliaras George G., *Adv. Mater.* **2017**, *29*, 1701217.
[14] D. T. Simon, K. C. Larsson, D. Nilsson, G. Burström, D. Galter, M. Berggren, A. Richter-Dahlfors, *Biosens. Bioelectron.* **2015**, *71*, 359.

[15] T. Yang, S. Hakimian, T. H. Schwartz, *Epileptic. Disord.* **2014**, *16*, 271.
[16] I. S. Fernández, T. Loddenkemper, *J. Clin. Neurophysiol.* **2013**, *30*, 554.
[17] D. Khodagholy, J. N. Gelinas, T. Thesen, W. Doyle, O. Devinsky, G. G. Malliaras, G. Buzsáki, *Nat. Neurosci.* **2015**, *18*, 310.
[18] D. Khodagholy, J. N. Gelinas, G. Buzsáki, *Science* **2017**, *358*, 369.
[19] G. Kozák, A. Berényi, *Sci. Rep.* **2017**, *7*, 6300.
[20] J. Yu, Y. Zhang, J. Yan, A. R. Kahkoska, Z. Gu, *Int. J. Pharm.* **2018**, *544*, 350.
[21] C. M. Proctor, J. Rivnay, G. G. Malliaras, *J. Polym. Sci. Part B Polym. Phys.* **2016**, *54*, 1433.
[22] P. T. Francis, *CNS Spectr.* **2005**, *10*, 6.
[23] G. C. Mathews, *Epilepsy Curr.* **2007**, *7*, 28.
[24] A. B. Hjelmeland, Q. Wu, J. M. Heddleston, G. S. Choudhary, J. MacSwords, J. D. Lathia, R. McLendon, D. Lindner, A. Sloan, J. N. Rich, *Cell Death Differ.* **2011**, *18*, 829.
[25] K. A. Lindsey, R. O. Brown, G. O. Maish, M. A. Croce, G. Minard, R. N. Dickerson, *Nutr. Burbank Los Angel. Cty. Calif* **2010**, *26*, 784.
[26] E. O. Gabrielsson, P. Janson, K. Tybrandt, D. T. Simon, M. Berggren, *Adv. Mater.* **2014**, *26*, 5143.
[27] T. Arbring Sjöström, A. Jonsson, E. Gabrielsson, L. Kergoat, K. Tybrandt, M. Berggren, D. T. Simon, *ACS Appl. Mater. Interfaces* **2017**, *9*, 30247.
[28] E. Stavrinidou, P. Leleux, H. Rajaona, D. Khodagholy, J. Rivnay, M. Lindau, S. Sanaur, G. G. Malliaras, *Adv. Mater.* **2013**, *25*, 4488.
[29] D. A. Koutsouras, P. Gkoupidenis, C. Stolz, V. Subramanian, G. G. Malliaras, D. C. Martin, *ChemElectroChem* **2017**, *4*, 2321.
[30] I. Uguz, M. Ganji, A. Hama, A. Tanaka, S. Inal, A. Youssef, R. M. Owens, P. P. Quilichini, A. Ghestem, C. Bernard, S. A. Dayeh, G. G. Malliaras, *Adv. Healthc. Mater.* **2016**, *5*, 3094.
[31] L. C. Wong-Kisiel, T. Blauwblomme, M.-L. Ho, N. Boddaert, J. Parisi, E. Wirrell, R. Nabbout, *Epilepsy Res.* **2018**, *145*, 1.
[32] R. Guerrini, M. Duchowny, P. Jayakar, P. Krsek, P. Kahane, L. Tassi, F. Melani, T. Polster, V. M. Andre, C. Cepeda, D. A. Krueger, J. H. Cross, R. Spreafico, M. Cosottini, J. Gotman, F. Chassoux, P. Ryvlin, F. Bartolomei, A. Bernasconi, H. Stefan, I. Miller, B. Devaux, I. Najm, F. Giordano, K. Vonck, C. Barba, I. Blumcke, *Epilepsia* **2015**, *56*, 1669.
[33] M. Szente, A. Baranyi, *Brain Res.* **1987**, *413*, 368.
[34] H. Pasantes-Morales, M. E. Arzate, O. Quesada, R. J. Huxtable, *Neuropharmacology* **1987**, *26*, 1721.
[35] D. J. Poxson, M. Karady, R. Gabrielsson, A. Y. Alkattan, A. Gustavsson, S. M. Doyle, S. Robert, K. Ljung, M. Grebe, D. T. Simon, M. Berggren, *Proc. Natl. Acad. Sci.* **2017**, *114*, 4597.
[36] S. D. Adams, A. Z. Kouzani, S. J. Tye, K. E. Bennet, M. Berk, *J. NeuroEngineering Rehabil.* **2018**, *15*, 8.
[37] M. T. Salam, M. Mirzaei, M. S. Ly, D. K. Nguyen, M. Sawan, *IEEE Trans. Neural Syst. Rehabil. Eng.* **2012**, *20*, 432.
[38] E. Z. Mangubat, R. G. Kellogg, T. J. Harris, M. A. Rossi, *J. Neurosurg.* **2015**, *122*, 1283.

The table of contents entry

Design concepts from state-of-the-art devices for recording activity on the surface of the brain and for delivering drugs with excellent spatiotemporal control are combined into a single multifunctional device. These findings represent a significant step forward in the development of cortical drug-delivery systems.

Keyword: bioelectronics, electrophoresis, drug delivery, electrocorticography

Christopher M. Proctor[1,5,q], Ilke Uguz[2,5,q], Andrea Slezia[3], Vincenzo Curto[1,5], Sahika Inal[4,5], Adam Williamson[3], and George Malliaras[1,4]*

Title An electrocorticography device with an integrated microfluidic ion pump for simultaneous neural recording and drug delivery *in vivo*

ToC figure

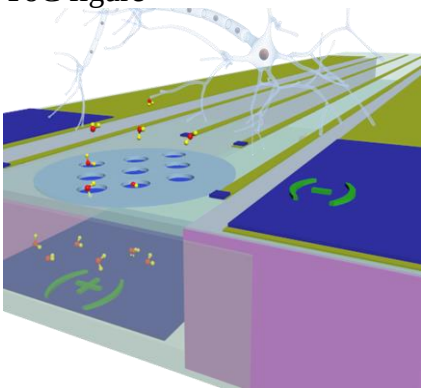

Supporting Information

An electrocorticography device with an integrated microfluidic ion pump for simultaneous neural recording and electrophoretic drug delivery *in vivo*

Christopher M. Proctor[1,5,+], Ilke Uguz[2,5,+], Andrea Slezia[3], Vincenzo Curto[1,5], Sahika Inal[4,5], Adam Williamson[3], and George Malliaras[1,4*]*

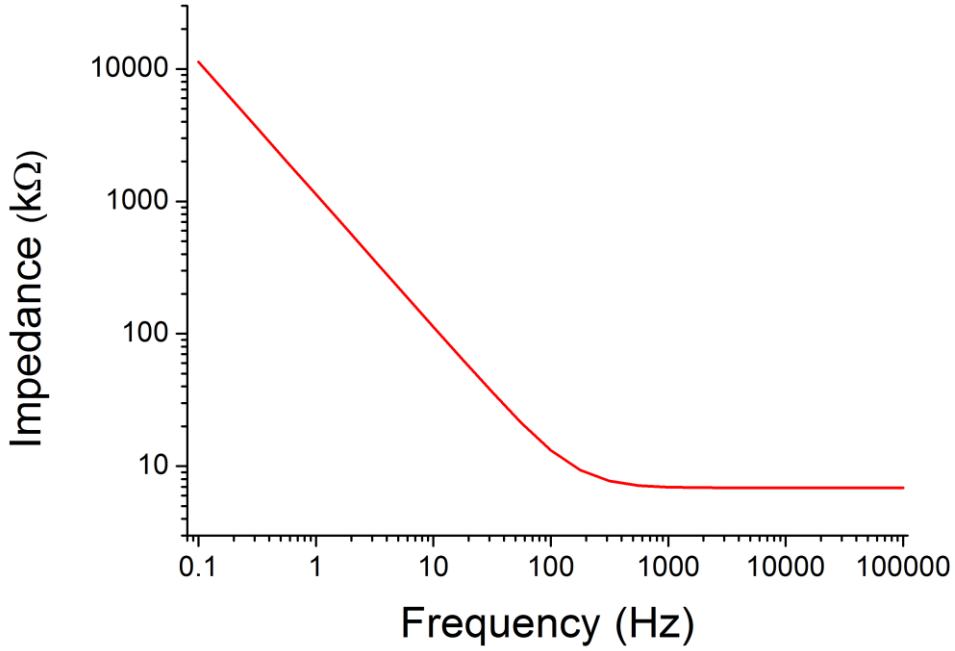

Figure S1. Impedance of a typical PEDOT:PSS coated recording site in the active area

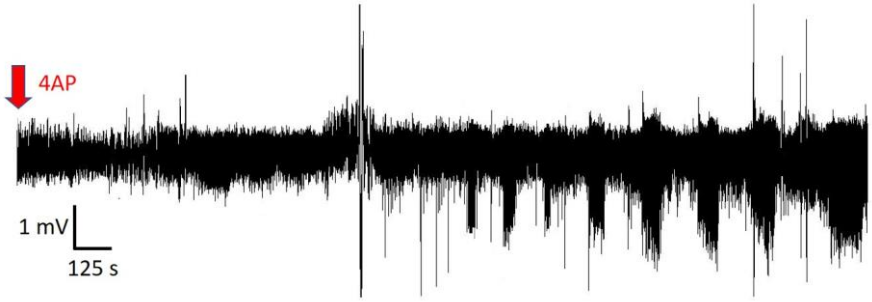

Figure S2. Representative of 4AP induced SLEs without uFIP treatment.